IEEE Access
Multidisciplinary | Rapid Review | Open Access Journal

Received December 21, 2018, accepted December 24, 2018, date of publication January 9, 2019, date of current version February 8, 2019.

Digital Object Identifier 10.1109/ACCESS.2019.2891909

160-GHz Radar Proximity Sensor With Distributed and Flexible Antennas for Collaborative Robots

MARTIN GEIGER, (Student Member, IEEE), AND CHRISTIAN WALDSCHMIDT, (Senior Member, IEEE)
Institute of Microwave Engineering, Ulm University, 89081 Ulm, Germany
Corresponding author: Martin Geiger (martin-2.geiger@uni-ulm.de)

This work was supported in part by the Ministry for Science, Research, and Arts Baden-Württemberg through the Project ZAFH MikroSens.

ABSTRACT There is a growing demand for collaborative robots in order to improve the efficiency of industrial processes and to push Industry 4.0 forward. The challenge for these robots is the compliance of the safety regulations to protect human workers from injuries. Therefore, a large number of sensors for the close range (several centimeters up to some meters) around the robot are needed. For a protective cover around the robotic arms all sensors must cooperate and process their information together. This paper presents a close range proximity sensor based on a 160-GHz radar MMIC with a transition to two flexible dielectric waveguides. On the low-loss waveguides, leaky-wave antennas with a large field of view are distributed. This reduces the number of sensors and achieves a coverage area for one sensor of more than 2200 cm^2 for a distance of 30 cm. For distances below 30 cm the sensor has blind areas. However, the expected extended targets like body parts can still be detected and the proximity sensor will stop the robot in the danger area. Additionally, the flexible waveguide offers the possibility to place the antennas almost arbitrarily around the robotic arm. For a single target scenario it is even possible to determine the target position by multilateration with only one receive channel.

INDEX TERMS Radar proximity sensor, millimeter wave, dielectric waveguide, antenna network, flexible antenna, Co-Bots.

I. INTRODUCTION

The collaboration of humans and robots plays an essential role in the improvement of modern industrial processes. Collaborative robots (Co-Bots), which are working directly together with humans, are able to relieve the employee and combine the skills of both partners: the speed, power, and repeatability of the robot and the problem solving competencies and adaptability of qualified humans [1]. However, the safety of the employee must be guaranteed with appropriate sensors around the robot. The safety system of the Co-Bot should avoid the collision with the human and stop the robot if a collision is unavoidable. For this purpose, a 360°-environment recognition of an approaching body part is desired.

There are already different commercially available safety systems for Co-Bots. A very simple one is usually already integrated within the robot. Here, a sensor measures the motor torque by sensing the current and the rotor position. If the robot hits an obstacle or a human the motor will stop because the current exceeds a preassigned threshold. A soft cover around the robot protects the human workers in case of a collision [2]. The disadvantage of this system is the unavoidable collision of Co-Bot and human. To avoid serious injuries the robot speed is limited and thereby, the advantages of collaboration are reduced.

Another safety system uses a sensor skin with more than 120 capacitive sensors [3]. They are able to measure distances up to several centimeters and stop the robot motor if an obstacle is within the sensing range. Due to the susceptibility of capacitive sensors to changing humidity, this sensor often requires a calibration in rough environments. Furthermore, only a small volume is monitored by this sensor and feasible evasive actions are not executable.

A further Co-Bot approach only assists the worker's movement and is controlled by a force-torque sensor or an

external joystick [4]. The robot is restricted to guided movements, and autonomous movements are only partly possible.

There are various other systems with combinations of protective skins and sensors like ultrasonic sensors, capacitive sensors or cameras for a complete environmental recognition. They combine the advantages of each system but require a higher sensor effort.

With a mm-wave radar it is possible to measure distances and velocities independently from environmental impacts like heavy weather conditions or lighting and by the integration of complete radar systems on an MMIC it becomes low-cost [5]–[7]. With more complex radar systems like phased arrays [8], [9] or MIMO approaches [10]–[12] it is even possible to estimate the angle of a target. Thereby, the signals from several antennas spaced by $\lambda/2$ are measured. By evaluating the phase difference between them the target angle can be estimated. Another way to measure a target position is a multilateration approach with distributed radar sensors [13]. Consequently, the fusion of several radar sensors provides a full 360°-environment surveillance system. A draw-back is the large number of single radar sensors and the high effort to combine the individual captured radar data.

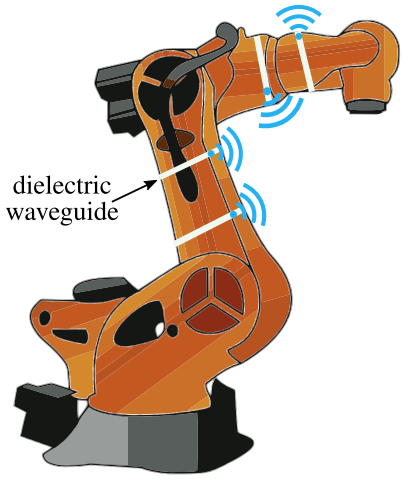

FIGURE 1. Schematic view on a robot with a radar safety system. The flexible waveguide is positioned around the robotic arms.

Instead of using many separated radar sensors, it would be advantageous to use less sensors and distribute antennas over the surface of the robot. With this approach the same spatial coverage can be achieved as shown in Fig. 1. Therefore, a suitable feeding network with the ability to distribute mm-wave signals over a large distance around a robot is required. Consequently, an approach with a microstrip feeding network on PCB is useless since the substrate losses are too high and the substrate is not flexible, especially at mm-wave frequencies. Other common waveguides in the mm-wave range like metallic rectangular waveguides are also not flexible.

By using dielectric waveguides, a low-loss feeding would be possible [14], [15] and even broadside antennas like leaky-wave antennas can be realized on these waveguides [16], [17]. Furthermore, they are flexible and can be easily positioned around a robotic arm.

In this paper, a proximity sensor with distributed leaky-wave antennas on a dieletric waveguide made of high density polyethylen (HDPE) is presented. With the operation frequency of 160 GHz and a large absolute bandwidth, the position of a target can be determined with millimeter accuracy. In Chapter II the requirements for a proximity sensor and the radar system are presented. Afterwards, the antenna and the feeding network design are explained in detail. The fabrication process and the measurement results for the antenna and the radar operation are shown in the last chapter.

II. SYSTEM DESCRIPTION

For a proximity sensor an antenna system with a maximum spatial coverage should be designed. The monitored area should be exhaustive in 30 cm distance from the robotic arm. For regions closer to the robot, the sensor should stop it. Thereby, the robot can be slowed down fast enough despite a high velocity. The monitored area is limited by the 3 dB angular width of the antenna. This also means, that the proximity sensor is not completely blind for regions below 30 cm, but has just blind zones. Since an extended target like a human worker is expected, the minimum monitored distance is considerably closer to the robot.

With the striven large field of view the number of MMICs can be reduced to a minimum. Since the proximity sensor should stop the robot if a human is within the danger area the range resolution in the close range should be around 1 cm. Furthermore, the antennas should be flexible and movable to distribute them arbitrarily around the robotic arm. Besides, this offers the possibility to separate electronics and antennas spatially, which can be advantageous for robotic applications in harsh industrial environments.

The used radar system is based on a 160-GHz radar MMIC [18] and has a transition to flexible dielectric waveguides made of HDPE ($\varepsilon_{r,\mathrm{HDPE}} = 2.25$, $\tan\delta = 3.1 \cdot 10^{-4}$ at 160 GHz). The system concept is shown in Fig. 2.

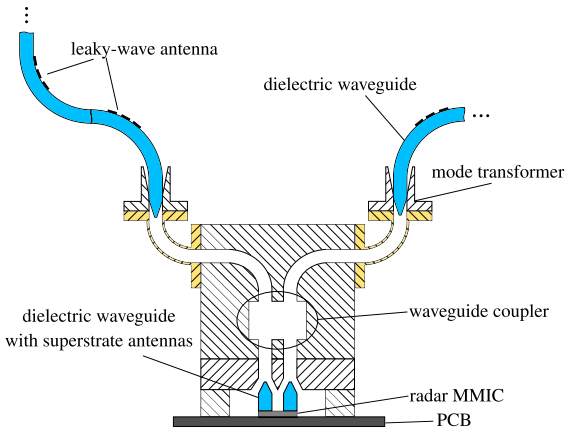

FIGURE 2. System concept of the 160-GHz radar MMIC with the transition to the flexible leaky-wave antennas.

The individual components which are needed for the transition from the radar MMIC to the dielectric waveguide are explained in detail in [19]. The bistatic radar MMIC architecture with a frequency offset synthesizer reduces the phase noise of the transmit signal. With a bandwidth of 16 GHz the range resolution of the radar MMIC is below 1 cm. Thus, the requirement for the high range resolution in the close range is fulfilled. The FMCW signal from the radar MMIC is radiated using an on-chip antenna. It consists of a shortened $\lambda/4$ patch with a 127 µm thick quartz glass superstrate, which is metallized with a $\lambda/2$ patch. On the superstrate a short dielectric rod antenna is positioned, which radiates the signal into a widened rectangular waveguide. The metallic waveguide block is galvanically isolated from the MMIC to avoid mechanical stress and to facilitate the assembly. The signal is equally divided by a wideband hybrid coupler in rectangular waveguide technology. The signals are fed to the dielectric waveguide using a mode transformer, which excites the fundamental HE_{11} mode. The complete transition from MMIC to dielectric waveguide has an insertion loss of 9.4 dB.

The dielectric waveguides with the leaky-wave antennas form the front-end of the radar system. With a rectangular cross section of 648 µm × 1295 µm the dielectric waveguide is bendable up to a radius of 1.5 cm with negligible radiation losses. The insertion loss of a straight waveguide is in the range of 4.5 dB/m at 160 GHz. This low loss waveguide is suitable to feed distributed antennas over a larger distance.

The before mentioned properties of the dielectric waveguide were determined for a waveguide with air ($\varepsilon_r = 1$) around it. If the waveguide is in contact to the metallic robot surface, the assumed condition with a surrounding material with dielectric constant of $\varepsilon_r < \varepsilon_{r,\mathrm{HDPE}}$ is not fulfilled anymore. Thus, a flexible coating around the waveguide is additionally needed. As material a HDPE foam (density $\rho = 30$ kg/m^3) [20] with a HDPE percentage of only 3% is used. The air inclusions decrease the dielectric constant, and the dielectric foam properties can be almost treated as air [21]. However, an additional loss of 1.5 dB/m was measured with the coating. This can be explained by additional material losses and mismatch.

III. ANTENNA AND FEEDING NETWORK

To achieve a maximum spatial coverage the antenna and the feeding network have to be investigated in detail. The design process is explained in the following sections.

A. LEAKY-WAVE ANTENNA

On a dielectric waveguide a wave travels along the guiding structure in x-direction. Through the placement of periodic metallic perturbations on the dielectric waveguide, radiating modes are excited like depicted in Fig. 3 [16]. Due to the extent in x-direction, the radiated beam is fan-shaped and directive in the x-z-plane. The width w of the metallic strip determines the radiated power per strip and the number of perturbations n defines the directivity and efficiency of

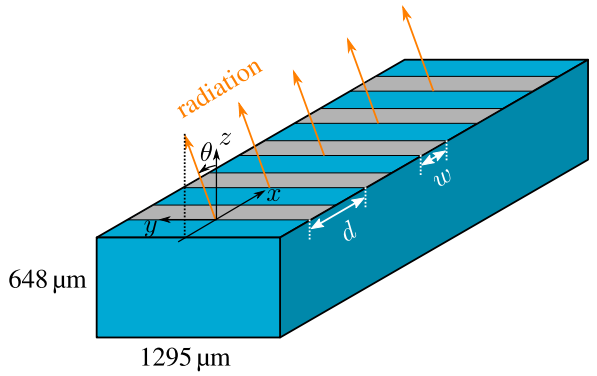

FIGURE 3. View on a dielectric leaky-wave antenna with rectangular cross-section and metallized grating [16].

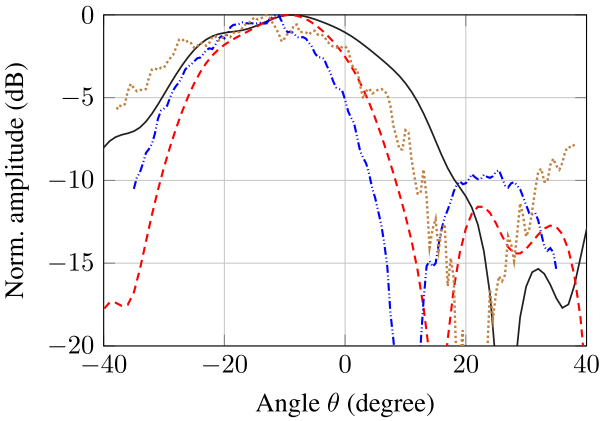

FIGURE 4. Simulated ($n = 2$ (——), $n = 3$ (– – –)) and measured ($n = 2$ (·····), $n = 3$ (–·–·–)) radiation patterns in the E-plane for different numbers of antennas.

the antenna. The leaky-wave antenna is frequency scanning since it is series fed. The beam direction moves from backward to forward with a stopband at broadside. The main beam angle depends on the strip spacing d.

Since the proximity sensor should use a minimum number of radar sensors, each antenna should have a maximum field of view. Therefore, antennas with only $n = 2$ and $n = 3$ perturbations, which have the largest field of view, are investigated in more detail by applying full wave simulations and measurements. In Fig. 4 the simulated and measured E-plane (x-z plane) radiation patterns are shown. Compared to the simulations, the measured radiation patterns are shifted by 4° due to inaccuracies in the measurement setup. For $n = 2$ the 3 dB angular width is 31° and the measured sidelobe level is larger than −8 dB. For $n = 3$ the 3 dB angular width decreases to 22.5°, and also the sidelobe level decreases below −9.5 dB. The H-plane has a 3 dB angular width of 63° for both antennas.

Besides the radiation pattern, the antenna gain should also be considered for the antenna design. The gain can be adjusted by the metallization width w. In Fig. 5 the simulated antenna gain with respect to the metallization width is shown for $n = 2$ and $n = 3$ perturbations. With increasing

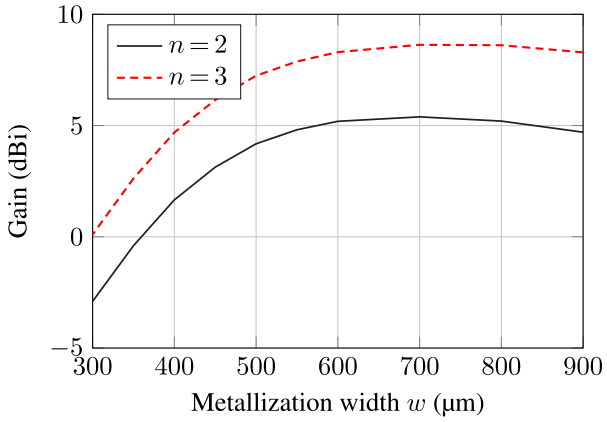

FIGURE 5. Antenna gain over metallization width with 2 and 3 perturbations.

metallization width the gain increases up to the width of $w \approx d/2$. For $n = 3$ the maximum gain is 8.6 dBi and about 3 dBi higher than for 2 perturbations. In the following only the antenna with 3 metal strips is investigated because of the lower sidelobe level and the higher gain compared to the smaller antenna.

B. FEEDING NETWORK

The monitored area and the power radiation per antenna must be considered for the arrangement of the antennas. For the spatial coverage the 3D-radiation pattern should be considered. Since the beam width in the y-z-plane is very broad, an almost constant beam in the 3 dB angular width for a straight dielectric waveguide is assumed. Also, the antennas are serial fed in the x-direction (E-plane). Therefore, only the antenna arrangement in the x-z-plane is investigated.

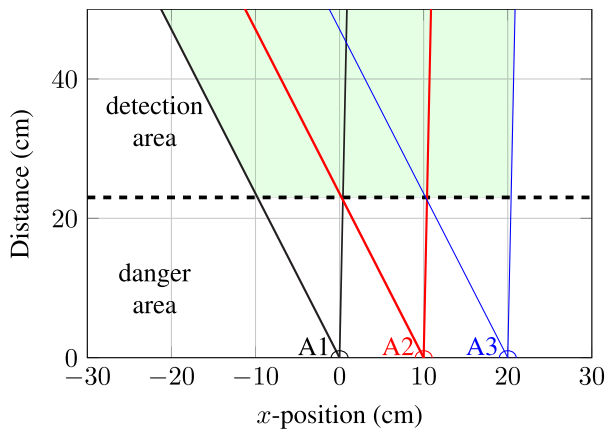

FIGURE 6. Monitored area (green colored) of the radar in the x-z-plane for an antenna spacing of 10 cm.

In order to avoid crosstalk and direct coupling between the antennas, the spacing between them should be larger than $50\lambda = 9.4$ cm. An exhaustive coverage in the required distance is achieved by using an antenna spacing of 10 cm as shown in Fig. 6. Here, the antenna positions and the individual 3 dB angular widths are depicted and the exhaustive monitored area (green color) is defined by the intersections of the beams. The achieved coverage is 30 cm in a distance of 24 cm for 3 antennas. Since the antennas are frequency scanning, the beam direction is shifted by 5° over the used frequency range of 10 GHz. However, the monitored area remains constant.

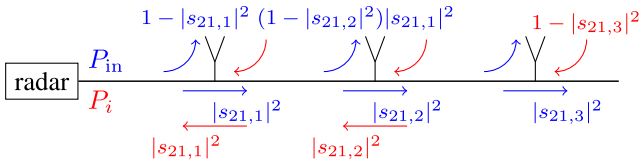

FIGURE 7. Radiated (blue) and received (red) power of serial fed antennas.

For the design of the metal strip width the serial feeding of the antennas as well as the different directivities D and material losses have to be considered. Each signal path in the antenna system with radiated and received power is shown in Fig. 7. The design goal is that the received power P_i from each antenna at the feeding point of the dielectric waveguide regardless of free-space propagation should be the same. This means that the last antenna should radiate most efficiently since less power is fed in ($|s_{21,1}|^2|s_{21,2}|^2\ P_{in}$) as well as additional dielectric 4.5 dB/m and radiation losses in the receive path attenuate the signal. The received power P_i from antenna i depends on the insertion loss $s_{21,i}$ of the antenna itself $\left(1-|s_{21,i}|^2\right)$ and the antennas between the radar and antenna i. With the input power P_{in} the received power P_i is

$$P_i = P_{in}\left(1-|s_{21,i}|^2\right)^2 \prod_{k=1}^{i-1}\left(|s_{21,k}|^2\right)^2. \tag{1}$$

From (1) the attenuation $L = P_i/P_{in}$ for each antenna can be determined. The signal is attenuated by L compared to an antenna system with 100% efficiency. As a result the important term for the radar equation can be determined by

$$G^2 = G_r G_t = LD^2. \tag{2}$$

The gain product G^2 is with respect to the dielectric waveguide feeding point. G_r is the receive antenna gain and G_t the transmit antenna gain. From the simulated antenna efficiencies the width for 3 serial fed antennas are determined to $w_1 = 350$ µm, $w_2 = 400$ µm, and $w_3 = 700$ µm. Considering the fabrication tolerances, the received power per antenna is nearly the same for these widths. Thus, the gain can be determined to $G_1^2 = 6.5$ dBi, $G_2^2 = 6.0$ dBi, and $G_3^2 = 7.7$ dBi. Disadvantageous of this feeding system is the trade-off between the large field of view and the efficiency of the antenna. Therefore, the antennas only radiate 60% of the input power resulting in $\prod_{k=1}^{3}|s_{21,k}| = -9$ dB.

With this antenna configuration the proposed system has an exhaustive coverage of 60 cm × 30 cm = 1800 cm^2 in a distance of 25 cm. As a comparison, an on-chip antenna with dielectric resonators with a 3-dB beamwidth of approximately 70° [18] has a coverage area

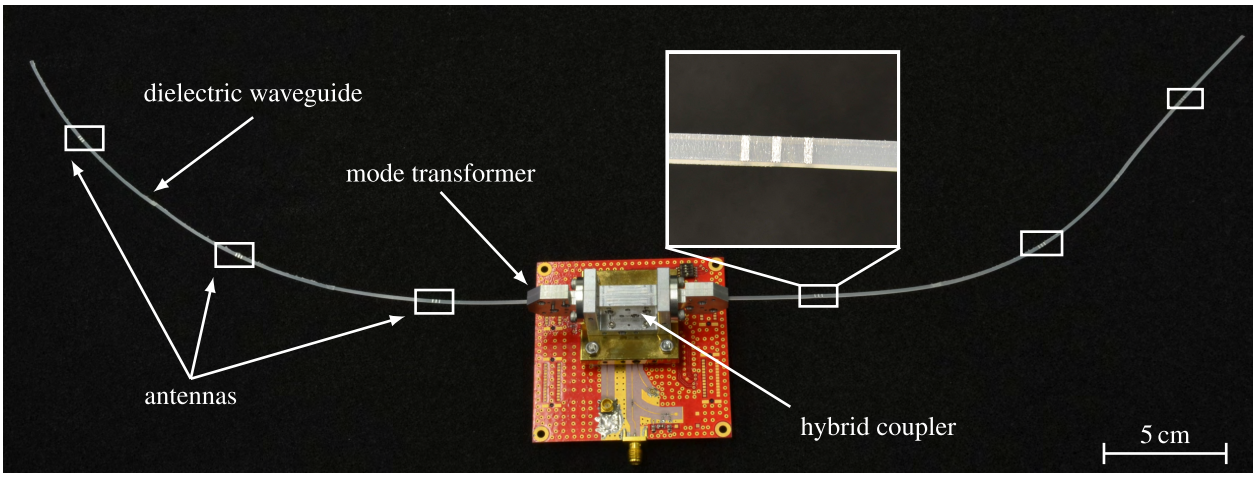

FIGURE 8. Radar proximity sensor with two dielectric waveguides and a detailed view on one antenna. The foam cover is removed for the photo.

of 36 cm × 36 cm = 1296 cm^2 for the same distance. Furthermore, the bendable waveguide offers additional degrees of freedom for the positioning of the PCB and the antennas at the robot. The antenna network and covered area can be extended to four or more antennas, dependent on the transmit power and receiver noise of the MMIC.

IV. FABRICATION AND MEASUREMENT RESULTS

A. FABRICATION

The leaky-wave antenna was fabricated in two steps. At first, the dielectric waveguide was milled to the waveguide dimensions from an HDPE plate. Afterwards the dielectric waveguide was metallized in a clean room process. The dielectric waveguide was metallized at the antenna positions with a 5 nm thick adhesion layer and a 100 nm thick aluminum layer. To metallize only the antenna positions, a mask with cavities at the perturbation positions was used. Due to the fabrication process, the maximum waveguide length is 10 cm. Therefore, the single waveguide pieces were glued together resulting in a final waveguide length of 30 cm comprising three single antennas. The proximity sensor with the dielectric waveguides and leaky-wave antennas is shown in Fig. 8. The foam coating was removed for the photo.

B. ANTENNA SYSTEM

In order to verify the feeding network with measurements, the S-parameters of the dielectric waveguide with antennas were determined. In Fig. 9 the reflection and transmission coefficient are shown. The calibration plane for the measurements is the waveguide flange of the mode transformer. In the operating range of the MMIC from 146 GHz to 162 GHz the reflection coefficient is below −10 dB. Above this frequency the leaky-wave antenna has the aforementioned stopband and radiates in broadside direction. The measured $|s_{21}|$ within the operating range is around −9 dB and corresponds well with the expected simulated values. The additional losses of the mode transformers (0.8 dB) are already de-embedded.

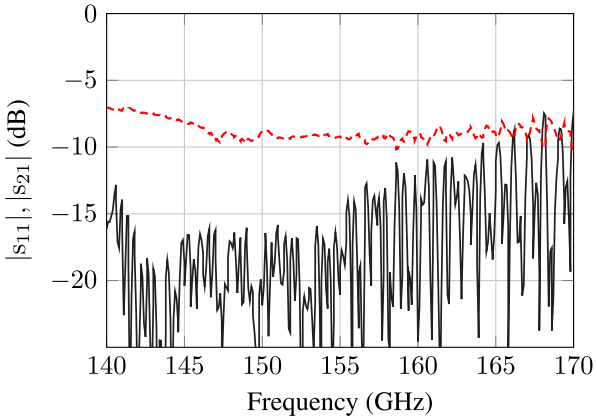

FIGURE 9. S-parameter measurement (s_{11} (——), s_{21} (- - - -)) for the feeding network with three leaky-wave antennas with the waveguide flange as calibration plane.

C. APPLICATION AND RADAR MEASUREMENTS

The application for the proximity sensor is to detect a human worker close to a Co-Bot and to stop it if someone enters the danger area. The system configuration with distributed antennas allows to place the dielectric waveguide arbitrarily around the robotic arm. Thereby, the MMIC on the PCB can be separated from the antennas and is protected from harsh environments. To investigate the performance of the proximity sensor, radar measurements were done for various system and target constellations. For all the measurements the antennas were positioned horizontally along the x-axis in a straight line. This simple but realistic scenario enables to explain and evaluate the measured scenario.

An FMCW radar with a ramp duration of 250 µs and a bandwidth of 10 GHz was used. For one range spectrum 512 ramps were recorded and processed by applying an FFT on each ramp. Subsequently, the single spectra were averaged coherently to decrease the noise floor. For calibration purposes the measurement of the empty room was subtracted from the time signal. During the measurements one or more

corner reflectors were moved along the x-axis to verify the simulations.

1) COMPLETE SYSTEM WITH A SINGLE TARGET

The first sensor to be measured is the presented sensor with two dielectric waveguides, each comprising three antennas. The measured range profile for a corner reflector in 80 cm vertical distance over antenna A1 (cf. Fig. 6) of the right dielectric waveguide is shown in Fig. 10. In the range spectrum different targets, which are distinguished according to their source, are marked. The first three peaks (□) result from the mismatch of the antenna and can be determined from the calibration measurement of the empty room. The single peak positions are located at a distance of 15 cm, 30 cm, and 45 cm. Compared to the physical distance of 10 cm the distance increases due to the slower propagation speed in the dielectric waveguide compared to free space.

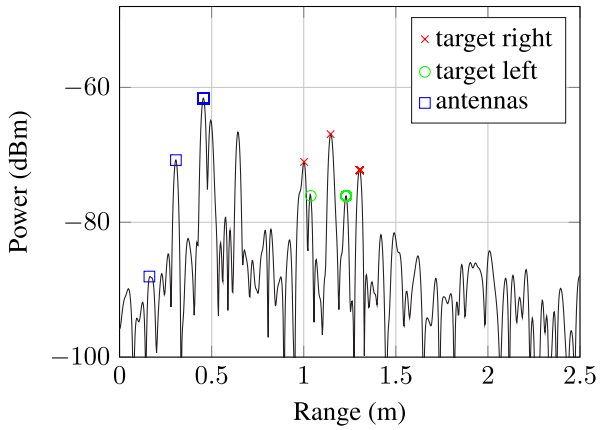

FIGURE 10. Measured range profile from the proximity sensor with both dielectric waveguides and a corner reflector over antenna A1 of the right dielectric waveguide.

Since each antenna radiates and receives a signal from a certain direction, the other targets can be assigned to the single antennas. All the antennas on the right dielectric waveguide illuminate the corner reflector and the three targets (×) can be assigned to these antennas. The other two targets (○) are measured by the first antennas of the left dielectric waveguide. A target from the third antenna on this waveguide is not seen as the beam does not illuminate the corner reflector. The additional target at 60 cm results from the attachment of the dielectric waveguide.

The allocation of the target peaks to the appropriate target and antenna can only be explained if there is a knowledge about the measured scenario. From the range profile it is only possible to recognize that one or more targets are near the robotic arm, which is sufficient information for a proximity sensor.

The minimum measurable distance for a proximity sensor is more important than determining the target positions. Since targets at a distance of 15 cm (30 cm) from antenna A1 and the mismatch reflection from antenna A2 (A3) result in an overlapping peak, the minimum unambiguous measurable distance between antenna A1 and the target is limited to 30 cm. With a more complex signal processing chain like target tracking, the minimum distance could be decreased. The calculated coverage area in x- and y-direction could be verified with measurements. The coverage area depends on the radar cross section of the target and exact measurements were only possible with corner reflectors.

2) ONE DIELECTRIC WAVEGUIDE WITH MULTIPLE TARGETS

For reasons of clarity only one dielectric waveguide was used in the following measurements. The second hybrid coupler port was terminated with a waveguide absorber. The end of the dielectric waveguide was matched with a transition to a rectangular waveguide and an absorber.

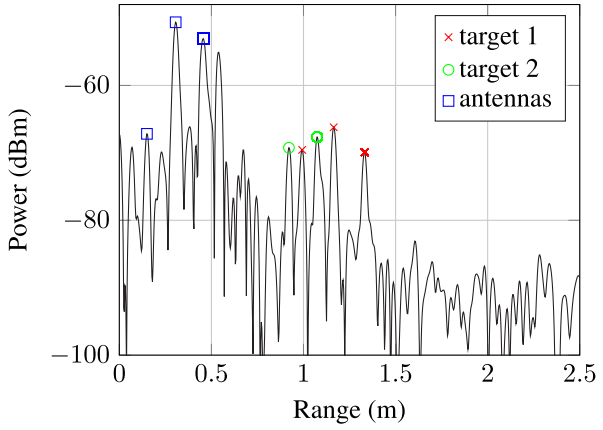

FIGURE 11. Measured range profile for two corner reflectors over antenna A1 (80 cm distance) and antenna A2 (50 cm distance).

In Fig. 11 a range profile of a radar measurement with two corner reflectors at different positions is shown. Target 1 was positioned 80 cm above antenna A1 and target 2 50 cm above antenna A2. Since target 1 is illuminated by all three antennas, three targets are visible in the range profile. Target 2 is only in the beam of antenna A2 and antenna A3. Consequently, only two targets can be measured. The first 3 targets result again from the antenna mismatch.

Also this information is only known due to the knowledge about the measured scenario. However, it is shown, that even a multiple target scenario can be detected by the sensor. With the complete sensor the range profile explanation with many targets would be too confusing. Therefore, only one dielectric waveguide was used in this scenario.

3) ONE DIELECTRIC WAVEGUIDE WITH ONE TARGET

The last shown measurement considers a special case. It was done using a single corner reflector as target, where even the target position can be determined. The measured range profile for a scenario with the corner reflector in $z = 1$ m distance vertically over antenna A1 is shown in Fig. 12. In this range profile three different targets and three different reflections are visible. The three antenna reflections result from

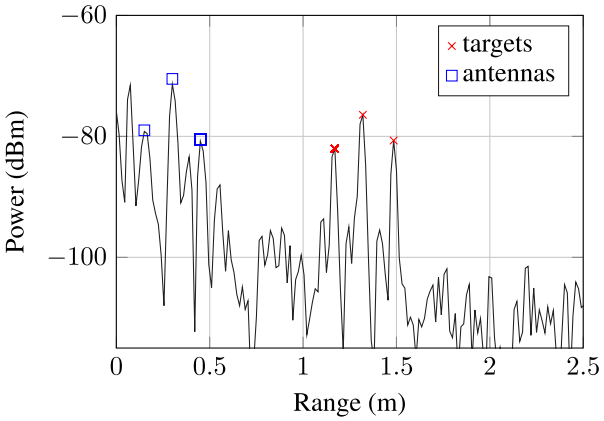

FIGURE 12. Measured range profile for a corner reflector in 1 m distance to antenna A1.

the mismatch of each antenna. As each antenna illuminates the corner reflector, the three target peaks can be assigned to the three corresponding antennas and the three distances $r_i = t_i - a_i$ from the antennas to the target can be determined. For the measured scenario the distances were calculated to $r_1 = 1.008$ m, $r_2 = 1.011$ m, and $r_3 = 1.035$ m.

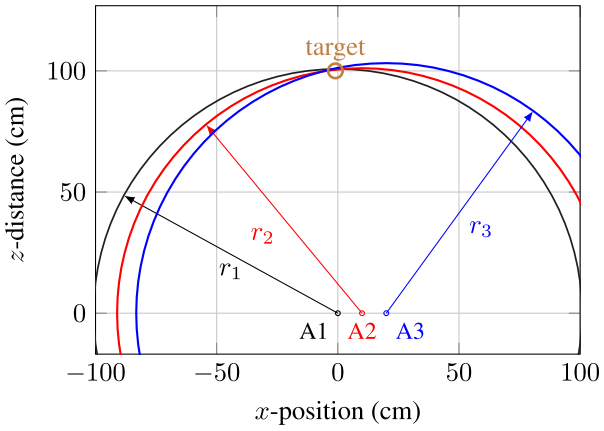

FIGURE 13. Target position calculation with multilateration for a single target scenario.

With this information multilateration can be used to calculate the target position in the x-z-plane for the case of a single target scenario. As depicted in Fig. 13, a circle with radius r_i is drawn around antenna i to determine the corner reflector position. The target position results from the intersection point between the three circles. Due to inaccuracies in the positioning of the target and the dielectric waveguide, the glueing connection of the antennas, and a slight torsion of the dielectric waveguide, there are three different intersection points. The centroid of this triangle is 4 cm shifted in $-x$-direction.

V. CONCLUSION

In this paper a 160-GHz radar proximity sensor with distributed flexible antennas for Co-Bot environment monitoring is presented. The large coverage area reduces the required number of sensors and the flexible antennas offer more degrees of freedom to position the antennas and sensors around the robot surface.

The radar system consists of a 160-GHz radar MMIC with a transition to two flexible dielectric waveguides. On each waveguide there are three leaky-wave antennas with $n = 3$ perturbations. The antennas are metallized in a distance of 10 cm from each other and the feeding system has an efficiency of 60%. For six antennas an exhaustive coverage is possible in a minimum distance of 30 cm with a monitored area of more than 2200 cm^2. Compared to an MMIC with on-chip antennas, the number of sensors can be reduced by more than 25%.

For the different investigated scenarios with single and multiple targets the sensor detects the targets and their range. For a single target scenario with only one dielectric waveguide even the target position can be determined with multilateration.

A further step to a sensor system would be the combination of several sensors around the robotic arms. Instead of using multilateration to determine the target position, a different approach might even solve the ambiguities.

ACKNOWLEDGMENT

The authors would like to thank Leuze electronic for the fruitful discussions and Rudolf Rösch from Institute of Optoelctronics, Ulm University, for the technical support.

REFERENCES

[1] F. Tobe. (Dec. 2015). *Why Co-Bots Will Be a Huge Innovation and Growth Driver for Robotics Industry*. [Online]. Available: https://spectrum.ieee.org/automaton/robotics/industrial-robots/collaborative-robots-innovation-growth-driver

[2] European Editors. (Aug. 2016). *Rise of the Cobots Inspires Safety Innovation*. [Online]. Available: https://www.digikey.co.nz/en/articles/techzone/2016/aug/rise-of-the-cobots-inspires-safety-innovation

[3] Robert Bosch GmbH. (Oct. 2018). *Human-Robot Collaboration*. [Online]. Available: https://www.bosch-apas.com/en/human-robot-collaboration/

[4] MRK-Systeme. (Oct. 2018). *Safeguiding*. [Online]. Available: https://www.mrk-systeme.de/produkt/features-safeguiding

[5] J. Hasch, E. Topak, R. Schnabel, T. Zwick, R. Weigel, and C. Waldschmidt, "Millimeter-Wave Technology for Automotive Radar Sensors in the 77 GHz Frequency Band," *IEEE Trans. Microw. Theory Techn.*, vol. 60, no. 3, pp. 845–860, Mar. 2012.

[6] R. Lachner, "Industrialization of mmWave SiGe technologies: Status, future requirements and challenges," in *Proc. IEEE 13th Top. Meeting Silicon Monolithic Integr. Circuits RF Syst.*, Jan. 2013, pp. 105–107.

[7] J. C. Scheytt *et al.*, "Towards mm-wave System-On-Chip with integrated antennas for low-cost 122 and 245 GHz radar sensors," in *Proc. IEEE 13th Top. Meeting Silicon Monolithic Integr. Circuits RF Syst.*, Jan. 2013, pp. 246–248.

[8] J. H. G. Ender *et al.*, "Progress in phased-array radar applications," in *IEEE MTT-S Int. Microw. Symp. Dig.*, Jun. 2005, p. 4.

[9] E. Brookner, "Developments and breakthroughs in radars and phased-arrays," in *Proc. IEEE Radar Conf. (RadarConf)*, May 2016, pp. 1–6.

[10] E. Fishler, A. Haimovich, R. Blum, D. Chizhik, L. Cimini, and R. Valenzuela, "MIMO radar: An idea whose time has come," in *Proc. IEEE Radar Conf.*, Apr. 2004, pp. 71–78.

[11] P. Hügler, F. Roos, M. Schartel, M. Geiger, and C. Waldschmidt, "Radar taking off: New capabilities for UAVs," *IEEE Microw. Mag.*, vol. 19, no. 7, pp. 43–53, Nov./Dec. 2018.

[12] H. J. Ng and D. Kissinger, "Highly miniaturized 120-GHz SIMO and MIMO radar sensor with on-chip folded dipole antennas for range and angular measurements," *IEEE Trans. Microw. Theory Techn.*, vol. 66, no. 6, pp. 2592–2603, Jun. 2018.

[13] F. Folster, H. Rohling, and U. Lubbert, "An automotive radar network based on 77 GHz FMCW sensors," in *Proc. IEEE Int. Radar Conf.*, May 2005, pp. 871–876.
[14] W. Volkaerts, N. Van Thienen, and P. Reynaert, "An FSK plastic waveguide communication link in 40 nm CMOS," in *IEEE ISSCC Dig. Tech. Papers*, Feb. 2015, pp. 1–3.
[15] S. Fukuda *et al.*, "A 12.5+12.5 Gb/s full-duplex plastic waveguide interconnect," *IEEE J. Solid-State Circuits*, vol. 46, no. 12, pp. 3113–3125, Dec. 2011.
[16] M. Geiger, M. Hitzler, and C. Waldschmidt, "A flexible dielectric leaky-wave antenna at 160 GHz," in *Proc. 47th Eur. Microw. Conf. (EuMC)*, Oct. 2017, pp. 240–243.
[17] A. Basu and T. Itoh, "Dielectric waveguide-based leaky-wave antenna at 212 GHz," *IEEE Trans. Antennas Propag.*, vol. 46, no. 11, pp. 1665–1673, Nov. 1998.
[18] M. Hitzler *et al.*, "Ultracompact 160-GHz FMCW radar MMIC with fully integrated offset synthesizer," *IEEE Trans. Microw. Theory Techn.*, vol. 65, no. 5, pp. 1682–1691, May 2017.
[19] M. Geiger, M. Hitzler, S. Saulig, J. Iberle, P. Hügler, and C. Waldschmidt, "A 160-GHz radar with flexible antenna used as a sniffer probe," *IEEE Sensors J.*, vol. 17, no. 16, pp. 5104–5111, Aug. 2017.
[20] "PE-Trobloc, Polyethylen-Weichschaumstoff," Gaugler & Lutz oHG, Aalen-Ebnat, Germany, Tech. Rep. DE 2014 V02, Oct. 2014.
[21] M. Stråt, I. Chmutin, and A. Boldizar, "Dielectric properties of polyethylene foams at medium and high frequencies," *Annu. Trans. Nordic Rheology Soc.*, vol. 18, no. 1, pp. 107–116, Apr. 2010.

MARTIN GEIGER (S'16) received the M.Sc. degree from Ulm University, Ulm, Germany, in 2015, where he is currently pursuing the Ph.D. degree.

In 2016, he joined the Institute of Microwave Engineering, Ulm University. His current research interests include novel radar sensor concepts with flexible antennas, dielectric waveguides, and MMIC interconnects, all at millimeter-wave frequencies.

Mr. Geiger was a recipient of the Best Student Paper Award at the 2018 International Microwave Symposium.

CHRISTIAN WALDSCHMIDT (S'01–M'05–SM'13) received the Dipl.Ing. (M.S.E.E.) and Dr.Ing. (Ph.D.E.E.) degrees from the University Karlsruhe (TH), Karlsruhe, Germany, in 2001 and 2004, respectively. From 2001 to 2004, he was a Research Assistant with the Institut für Höchstfrequenztechnik and Elektronik, Universität Karlsruhe (TH), Germany. Since 2004, he has been with the business units Corporate Research and Chassis Systems, Robert Bosch GmbH. He has been the Head of different research and development teams in microwave engineering, RF-sensing, and automotive radar.

In 2013, he returned to academia. He was appointed as a Full Professor and the Director of the Institute of Microwave Engineering, Ulm University, Germany. He has authored or co-authored over 140 scientific publications and more than 20 patents. His research interests include radar and RF-sensing, mm-wave and submillimeter-wave engineering, antennas and antenna arrays, and RF and array signal processing. He is the Executive Committee Board Member of the German MTT/AP Joint Chapter and a member of the ITG Committee Microwave Engineering (VDE). In 2015 and 2017, he served as the TPC Chair and, in 2018, as the Chair for the IEEE MTT International Conference on Microwaves for Intelligent Mobility. He is also the Chair of the IEEE MTT-27 Technical Committee (wireless enabled automotive and vehicular applications). Since 2018, he has been serving as an Associate Editor for the IEEE MTT Microwave Wireless Components Letters. He is a Reviewer for multiple IEEE Transactions and several conferences, including IMS and EUMW.